Quantum Light in Coupled Interferometers for Quantum Gravity Tests

I. Ruo Berchera,[1] I. P. Degiovanni,[1] S. Olivares,[2] and M. Genovese[1]

[1]*INRIM, Strada delle Cacce 91, I-10135 Torino, Italy*

[2]*Dipartimento di Fisica, Università degli Studi di Milano, and CNISM UdR Milano Statale, Via Celoria 16, I-20133 Milano, Italy*

(Received 22 January 2013; published 21 May 2013)

In recent years quantum correlations have received a lot of attention as a key ingredient in advanced quantum metrology protocols. In this Letter we show that they provide even larger advantages when considering multiple-interferometer setups. In particular, we demonstrate that the use of quantum correlated light beams in coupled interferometers leads to substantial advantages with respect to classical light, up to a noise-free scenario for the ideal lossless case. On the one hand, our results prompt the possibility of testing quantum gravity in experimental configurations affordable in current quantum optics laboratories and strongly improve the precision in ''larger size experiments'' such as the Fermilab holometer; on the other hand, they pave the way for future applications to high precision measurements and quantum metrology.

DOI: 10.1103/PhysRevLett.110.213601 PACS numbers: 42.50.St, 03.65.Ud, 04.60.−m, 42.25.Hz

The dream of building a theory unifying general relativity and quantum mechanics, the so-called quantum gravity, has been a key element in theoretical physics research for the past 60 years. Several attempts in this sense have been considered. However, for many years no testable prediction emerged from these studies, leading to the common wisdom that this kind of research was more properly a part of mathematics than of physics, being by construction unable to produce experimentally testable predictions as required by the Galilean scientific method. In the past few years this common wisdom has been challenged [1–6]. More recently, effects in interferometers connected to noncommutativity of position variables in different directions [7,8] have been considered for both cavities with microresonators [4] and two coupled interferometers [5], the so-called ''holometer.'' In particular, this last idea led to the planning of a double 40 m interferometer at Fermilab [9].

Here, we consider whether the use of quantum correlated light beams in coupled interferometers could lead to significant improvements allowing an actual simplification of the experimental apparatuses to probe the noncommutativity of position variables. On the one hand, our results demonstrate that the use of quantum correlated light can lead to substantial advantages in interferometric schemes also in the presence of nonunit quantum efficiency, up to a noise-free scenario for the ideal lossless case. This represents a big step forward with respect to the quantum metrology schemes reported in the literature [10–13], and paves the way for future metrology applications. On the other hand, they prompt the possibility of testing quantum gravity in experimental configurations affordable in a traditional quantum optics laboratory with current technology.

The idea at the basis of the holometer is that noncommutativity at the Planck scale ($l_p = 1.616 \times 10^{-35}$ m) of position variables in different directions leads to an additional phase noise, referred to as holographic noise (HN). In a single interferometer I this noise substantially confounds with other sources of noise, even though the most sensible gravitational wave interferometers are considered [5], since their HN resolution is worse than their resolution to gravitational wave at low frequencies. Nonetheless, if the two equal interferometers I_1 and I_2 of the holometer have overlapping spacetime volumes, then the HN between them is correlated and easier to identify [5]. Indeed, the ultimate limit for holometer sensibility, as for any classical-light based apparatus, is dictated by the shot noise; therefore, the possibility of going beyond this limit by exploiting quantum optical states is of the greatest interest [11,14–16].

In the past the possibility of exceeding the shot-noise limit in gravitational-wave detectors was suggested [17,18] and, recently, realized [19] by using squeezed light. As shown in the following, this resource can indeed allow an improvement of holometerlike apparatuses as well. Nonetheless, in this case, having two coupled interferometers, the full exploitation of properties of quantum light, and in particular of entanglement, may lead to much larger improvements.

In general, the observable measured at the output of the holometer may be described by an appropriate operator $\hat{C}(\phi_1, \phi_2)$, ϕ_k being the phase shift (PS) detected by I_k, $k=1, 2$, with expectation value $\langle \hat{C}(\phi_1, \phi_2)\rangle = \mathrm{Tr}[\rho_{12}\hat{C}(\phi_1, \phi_2)]$, where ρ_{12} is the overall density matrix associated with the state of the light beams injected in I_1 and I_2.

In order to observe the HN, one should compare [5] $\langle \hat{C}(\phi_1, \phi_2)\rangle$ in two different experimental configurations of I_1 and I_2, namely, parallel ($\parallel$) and perpendicular ($\perp$) (Fig. 1). In configuration $\parallel$, the interferometers are oriented so that the HN induces the same random fluctuation of their PSs, leading to a substantial correlation between them, since they occupy overlapping spacetime volumes [5,20]. Thus, by measuring the correlation of the

 © 2013 American Physical Society

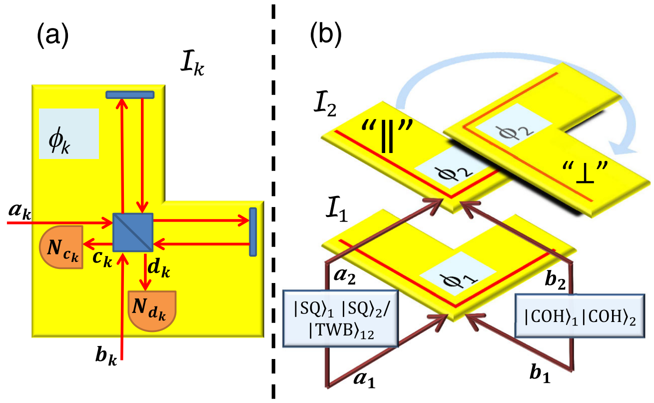

FIG. 1 (color online). Sketch of the holometer. (a) The two involved interferometers, I_k, $k = 1, 2$, have input modes a_k and b_k and output modes $c_k \equiv c_k(\phi_k)$ and $d_k \equiv d_k(\phi_k)$, where two detectors are placed for measuring the number of photons $\hat{N}_{c_k}(\phi_k)$ and $\hat{N}_{d_k}(\phi_k)$, respectively. (b) The interferometers are set in the configurations $\|$ and $\perp$ according to the picture. The input modes b_k, $k = 1, 2$, are always excited in two coherent states labeled as $|\mathrm{COH}\rangle_1|\mathrm{COH}\rangle_2$, while the modes a_k are excited in two uncorrelated squeezed vacua labeled as $|\mathrm{SQ}\rangle_1|\mathrm{SQ}\rangle_2$ [configuration (SQ)] or in a maximally entangled two-mode squeezed vacuum marked as $|\mathrm{TWB}\rangle_{12}$ [configuration (TWB)].

interference fringes, one can highlight the presence of the HN. Configuration $\perp$ serves as a reference measurement, namely, it corresponds to the situation where the correlation due to HN is absent, since their spacetime volumes are not overlapping [5,20]; in other words, it is equivalent to the estimation of the "background." The statistical properties of the PS fluctuations due to HN may be described by a suitable probability density function, $f_x(\phi_1, \phi_2)$, $x = \|, \perp$. In turn, the expectation of any operator $\hat{O}(\phi_1, \phi_2)$, or function of the PSs, should be averaged over f_x; namely,

$$\langle \hat{O}(\phi_1, \phi_2)\rangle \to \mathcal{E}_x[\hat{O}(\phi_1, \phi_2)] \equiv \int \langle \hat{O}(\phi_1, \phi_2)\rangle f_x(\phi_1, \phi_2) d\phi_1 d\phi_2. \quad (1)$$

As in the holometer, the HN arises as a correlation between two phases, the appropriate function to be estimated is their covariance in the parallel configuration $\mathcal{E}_{\|}[\delta\phi_1\delta\phi_2]$, where $\delta\phi_k = \phi_k - \phi_{k,0}$, and $\phi_{k,0}$ are the mean PS values measured by I_k, $k = 1, 2$. Since the holographic noise is supposed to be small, we can expand the $\hat{C}$ operator in terms of small fluctuation $\delta\phi_k$. According to Eq. (1) we are able to directly relate the covariance of the PSs to the observable quantities (see Supplemental Material, Sec. I, for details [21]):

$$\mathcal{E}_{\|}[\delta\phi_1\delta\phi_2] \approx \frac{\mathcal{E}_{\|}[\hat{C}(\phi_1, \phi_2)] - \mathcal{E}_{\perp}[\hat{C}(\phi_1, \phi_2)]}{\langle \partial^2_{\phi_1,\phi_2}\hat{C}(\phi_{1,0}, \phi_{2,0})\rangle}, \quad (\delta\phi_1, \delta\phi_2 \ll 1). \quad (2)$$

Equation (2) states that the covariance can be estimated by measuring the difference between the expectation values of the operator $\hat{C}$ in the two configurations. Thus, this difference represents the measured signal, while the coefficient at the denominator is the sensitivity.

One has to reduce as much as possible the uncertainty associated with its measurement:

$$\mathcal{U}(\delta\phi_1\delta\phi_2) \approx \sqrt{\frac{\mathrm{Var}_{\|}[\hat{C}(\phi_1, \phi_2)] + \mathrm{Var}_{\perp}[\hat{C}(\phi_1, \phi_2)]}{[\langle \partial^2_{\phi_1,\phi_2}\hat{C}(\phi_{1,0}, \phi_{2,0})\rangle]^2}}, \quad (\delta\phi_1, \delta\phi_2 \ll 1), \quad (3)$$

where $\mathrm{Var}_x[\hat{C}(\phi_1, \phi_2)] \equiv \mathcal{E}_x[\hat{C}^2(\phi_1, \phi_2)] - \mathcal{E}_x[\hat{C}(\phi_1, \phi_2)]^2$ [22]. We observe that the sum of variances derives from the independence of the two measurement configurations. Thanks to the same expansions leading to Eq. (2), we can write $\mathrm{Var}_x[\hat{C}(\phi_1, \phi_2)] = \mathrm{Var}[\hat{C}(\phi_{1,0}, \phi_{2,0})] + \mathcal{O}(\delta\phi^2)$ for both $x = \|, \perp$. Therefore, the zero-order contribution to the uncertainty is

$$\mathcal{U}^{(0)} = \frac{\sqrt{2\mathrm{Var}[\hat{C}(\phi_{1,0}, \phi_{2,0})]}}{|\langle \partial^2_{\phi_1,\phi_2}\hat{C}(\phi_{1,0}, \phi_{2,0})\rangle|}, \quad (4)$$

where $\mathrm{Var}[\hat{C}(\phi_{1,0}, \phi_{2,0})] = \langle \hat{C}(\phi_{1,0}, \phi_{2,0})^2\rangle - \langle \hat{C}(\phi_{1,0}, \phi_{2,0})\rangle^2$ does not depend on the PSs' fluctuations due to the HN, but it represents the intrinsic quantum fluctuations of the measurement described by the operator $\hat{C}(\phi_1, \phi_2)$ and depends on the optical quantum states sent in the holometer. In particular, our aim is to look for a suitable choice of quantum optical state ρ_{12} and an operator $\hat{C}(\phi_1, \phi_2)$ that reduces this zero-order contribution to the uncertainty. In the following we will demonstrate that the use of quantum resources, like squeezing or, much more, entanglement, provides huge advantages in terms of achieved accuracy with respect to classical light.

As a first example we consider a configuration (SQ) where the two input modes of each interferometer I_k, $k = 1, 2$, are excited in a coherent state and a squeezed vacuum state with mean number of photons μ_k and λ_k, respectively (see Fig. 1). Since the difference of the number of photons in the two output ports of each interferometer, $\hat{N}_{k-}(\phi_k) = \hat{N}_{c_k}(\phi_k) - \hat{N}_{d_k}(\phi_k)$, can be used to estimate the corresponding ϕ_k with sub-shot-noise resolution [10,11,17], reasonably the covariance $\mathcal{E}_{\|}[\delta\phi_1\delta\phi_2]$ can be efficiently evaluated from the covariance between $\hat{N}_{1-}(\phi_1)$ and $\hat{N}_{2-}(\phi_2)$. Therefore, we define $\hat{C}(\phi_1, \phi_2) = \Delta\hat{N}_{1-}(\phi_1)\Delta\hat{N}_{2-}(\phi_2)$, with $\Delta\hat{N}_{k-}(\phi_k) = \hat{N}_{k-}(\phi_k) - \mathcal{E}[\hat{N}_{k-}(\phi_k)]$ [we note that $\mathcal{E}_{\|}[\hat{N}_{k-}(\phi_k)] = \mathcal{E}_{\perp}[\hat{N}_{k-}(\phi_k)] = \mathcal{E}[\hat{N}_{k-}(\phi_k)]$, as a consequence of the properties of $f_x(\phi_1, \phi_2)$; see Supplemental Material, Sec. I [21]).

Figure 2 shows the corresponding uncertainty at the zero order given in Eq. (4): assuming identical input states ($\mu_k = \mu$ and $\lambda_k = \lambda$, $k = 1, 2$), the minimum is achieved

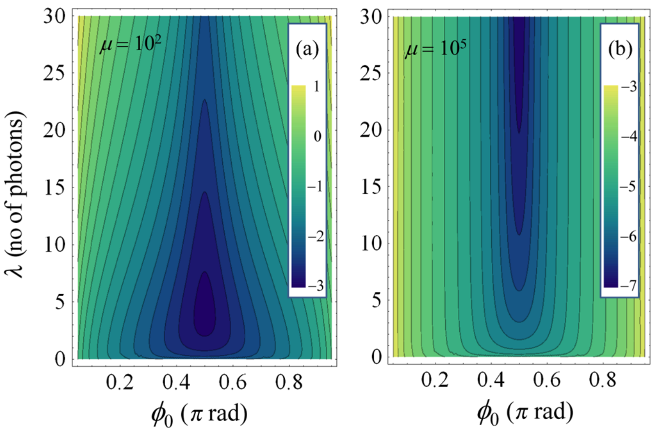

FIG. 2 (color online). The uncertainty of the phase covariance $\log_{10} \mathcal{U}_{\rm SQ}^{(0)}$ when the holometer is fed by two independent squeezed states plus two coherent fields. Here $\phi_{1,0} = \phi_{2,0} = \phi_0$ is the central PS of the interferometers, $\lambda_1 = \lambda_2 = \lambda$ is the intensity of each squeezing, $\mu_1 = \mu_2 = \mu$ is the intensity of each coherent beam, and their phase difference is set to zero. (a) $\mu \sim \lambda$, when the coherent and squeezed beams have similar intensities the noise reduction is lower bounded. (b) $\mu \gg \lambda$, in this regime quantum noise reduction increases with the amount of squeezing, offering a strong noise suppression if high level of squeezing can be reached. The region of the minimum runs at $\phi_0 = \pi/2$.

for $\phi_{1,0} = \phi_{2,0} = \pi/2$, and reads (see Supplemental Material, Sec. II [21])

$$\mathcal{U}_{\rm SQ}^{(0)}(\mu, \lambda) \approx \sqrt{2}\frac{\lambda + \mu\left(1 + 2\lambda - 2\sqrt{\lambda + \lambda^2}\right)}{(\lambda - \mu)^2}. \quad (5)$$

In perfect analogy with the PS measurement for a single interferometer [17,18], if $\mu \gg \lambda \gg 1$, then we have the optimal accuracy $\mathcal{U}_{\rm SQ}^{(0)} \approx (2\sqrt{2}\lambda\mu)^{-1}$. This represents a strong advantage in terms of uncertainty reduction [of the order $(4\lambda)^{-1}$] with respect to classical case $\mathcal{U}_{\rm CL}^{(0)} \approx \sqrt{2}/\mu$, i.e., when only coherent states are employed. Nevertheless, an important difference between the single interferometer PS measurement, involving a first-order moment of the photon number distribution, and the covariance estimation, involving the second-order momenta, arises: while in the first case the uncertainty scales as the usual standard quantum limit one, $\propto \mu^{-1/2}$, in the second case it scales $\propto \mu^{-1}$ (neglecting the little relative contribution of the squeezing to the intensity). We remark that the advantage of the present scheme is based on the independent improvement of the resolution of each interferometer which is itself limited by the amount of squeezing (see Supplemental Material, Sec. II [21]). However, the aim of the holometer is to couple I_1 and I_2 minimizing the noise on their outputs correlation, namely, regardless of the noise in the single interferometer. This suggests that quantum correlated states, coupling I_1 and I_2, could further enhance the performance of the holometer.

To this aim, we consider a new configuration (TWB) where modes a_1 and a_2 of Fig. 1 are excited in a continuous variable maximally entangled state, i.e., a two-mode squeezed vacuum state or twin-beam state, $|{\rm TWB}\rangle\rangle_{a_1,a_2} = S_{12}(\zeta)|0\rangle_{a_1,a_2} = \sum_{n=0}^{\infty} c_n(\zeta)|n\rangle_{a_1}|n\rangle_{a_2}$, where $S_{12}(\zeta) = \exp(\zeta a_1^\dagger a_2^\dagger - \zeta^* a_1 a_2)$ is the two-mode squeezing operator. This state can be easily produced experimentally, for example, by the parametric down-conversion process [23]. If we set $\zeta = |\zeta|e^{i\theta_\zeta}$ and introduce the mean photon number per mode $\lambda = \sinh^2|\zeta|$, then $c_n(\zeta) = (1+\lambda)^{-1/2}[(1+\lambda^{-1})e^{-i2\theta_\zeta}]^{-n/2}$ [24]. The input modes b_1 and b_2 are still excited in two coherent states, so that the four-mode input state is $|\psi\rangle = |{\rm TWB}\rangle\rangle_{a_1,a_2} \otimes |\alpha\rangle_{b_1} \otimes |\alpha\rangle_{b_2}$.

One of the peculiarities of the state $|{\rm TWB}\rangle\rangle_{a_1,a_2}$ is the presence of the same number of photons in the two modes [14,25–27], then each power of the photon number difference of the two modes is identically null, ${}_{a_1,a_2}\langle\langle{\rm TWB}|(\hat{N}_{a_1} - \hat{N}_{a_2})^M|{\rm TWB}\rangle\rangle_{a_1,a_2} = 0,\ \forall\ M > 0$.

We also observe that, in the absence of the HN and choosing the optimal working regime $\phi_{k,0} = 0$, $k = 1, 2$, I_1 and I_2 behave like two completely transparent media for their input fields [see again Supplemental Material, Sec. II, Eq. (4) [21]]. In particular, output modes c_1 and c_2 exhibit perfect correlation between the number of photons, which directly comes from the input modes a_1 and a_2, leading to the the natural choice of the observable as the fluctuation of the photon numbers' difference, $\hat{C}(\phi_1, \phi_2) = \Delta^2[\hat{N}_{c_1} - \hat{N}_{c_2}]$. Indeed, the numerator of Eq. (4), ${\rm Var}\{\Delta^2[\hat{N}_{c_1}(0) - \hat{N}_{c_2}(0)]\}$ is identically null, while the denominator reads

$$\langle\psi|\partial^2_{\phi_1,\phi_2}\Delta^2[\hat{N}_{c_1}(\phi_{1,0}) - \hat{N}_{c_2}(\phi_{2,0})]|\psi\rangle = -\frac{1}{2}\sqrt{\lambda(1+\lambda)}\mu\cos[2(\theta_\zeta - \theta_\alpha)], \quad (6)$$

which is nonzero for both $\lambda, \mu \neq 0$ and it is maximized for $\theta_\zeta - \theta_\alpha = 0$. This quantity represents also the coefficient of proportionality in Eq. (2) between the covariance of the HN and the measured signal. It is worth noting that, even though for $\phi_{k,0} = 0$ the coherent state gives no contribution to the output modes c_1 and c_2, being completely transmitted to the complementary modes d_1 and d_2, when fluctuations of the PS occurs a little portion will be reflected to the monitored ports and this guarantees the sensitivity to the HN PSs' covariance.

Thus, the correlation property of the TWB state leads to the amazing result that the contribution to the uncertainty coming from the photon number noise shown in Eq. (4) is $\mathcal{U}_{\rm TWB}^{(0)} = 0$ (when $\lambda, \mu \neq 0$), representing an ideal accuracy of the interferometric scheme to the PS's covariance due to HN and the main achievement of the present study.

The question that now arises is how and to what extent our conclusions are affected by a nonunity overall transmission-detection efficiency η (see Supplemental

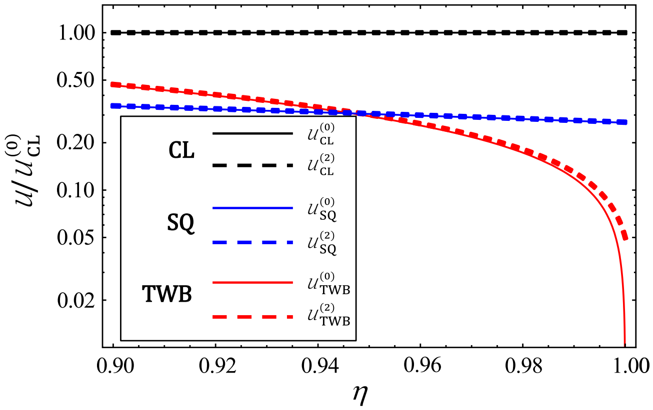

FIG. 3 (color online). Uncertainty reduction normalized to the classical limit $\mathcal{U}^{(0)}_{\rm CL}$ [30]. The solid lines represent the uncertainties only due to the photon noise, corresponding to the zero-order contribution [see Eq. (4)]. The coherent field intensity is set to $\mu = 2 \times 10^{23}$, while the twin beams and independent squeezed beam intensities are $\lambda_1 = \lambda_2 = \lambda = 0.5$. The dashed lines represent the second-order uncertainties including the RP contribution. For its calculation the measurement time is chosen $\tau = 10^{-3}$ s, the mirror mass $m = 10^2$ kg, and the central angular frequency of the light $\omega = 3.14 \times 10^{15}$ Hz (a wavelength of 600 nm.)

Material, Sec. III [21]). In Fig. 3 we plot $\mathcal{U}^{(0)}$ for the SQ, TWB and classical coherent state (CL) approaches, as a function of η (assumed to be the same for both the interferometers) for a modest level of nonclassical resources ($\lambda = 0.5$). As one may expect, SQ exhibits a small advantage in this regime. However, in the high efficiency region (albeit with values reasonably achievable with current technologies) the TWB-based approach provides a significant improvement not only with respect to classical setup, but also with respect to SQ.

Focusing on the limit of very small quantum resources, i.e., $\lambda \ll 1$ and $\mu \gg 1$, $\mathcal{U}^{(0)}_{\rm SQ}/\mathcal{U}^{(0)}_{\rm CL} \approx 1 - 2\eta\sqrt{\lambda}$ and $\mathcal{U}^{(0)}_{\rm TWB}/\mathcal{U}^{(0)}_{\rm CL} \approx \sqrt{2(1-\eta)/\eta}$. For a small amount of squeezing, the quantum noise $\mathcal{U}^{(0)}_{\rm SQ}$ not surprisingly approaches the classical case, while for TWB, we have a degradation of the performances with respect to the ideal case ($\eta = 1$). Anyway, an improvement with respect to the classical case is kept for $\eta > 2/3$, demonstrating that a relatively faint TWB can provide an interesting improvement in the HN detection.

In the opposite limit of high quantum resources exploited, i.e., $\mu \gg \lambda \gg 1$, $\mathcal{U}^{(0)}_{\rm SQ}/\mathcal{U}^{(0)}_{\rm CL} \approx (1-\eta) + \eta/(4\lambda)$ and $\mathcal{U}^{(0)}_{\rm TWB}/\mathcal{U}^{(0)}_{\rm CL} \approx 2\sqrt{5}(1-\eta)$ reveal that the performances of the quantum strategies are limited by the presence of the terms $(1-\eta)$. Here the main difference between SQ and TWB is that for $\eta \approx 1$ SQ exhibits an uncertainty lower bounded to $(4\lambda)^{-1}$, i.e., depending on the squeezing intensity. On the other hand, the TWB approach beats the classical one for $\eta > 0.683$, while for $\eta \approx 1$ it goes to zero: this demonstrates that the use of quantum light can largely improve the performances of a holometer addressed to test quantum gravity models.

A last source of noise, which could affect our results, may derive from the radiation pressure (RP) [17,28,29]. However, our model is perturbative in phase fluctuations $\delta\phi_k$ and, according to Eq. (4), the main noise contribution should come from the zeroth-order term corresponding to the photon noise. RP is assumed to introduce a second-order contribution to the uncertainty (see Supplemental Material, Sec. IV for details [21]) that is related to the light fluctuation in the arms of the interferometers and to the phase shift induced by the mirror's recoil [the latter is given by $(\omega\tau/2mc)\mathcal{P}$, where ω and $\mathcal{P}$ are the central frequency of the light and the momentum of the photon, respectively, τ the measurement time, and m the mirrors mass [17]]. In the case of a single interferometer fed by squeezed light, the amplitude of the RP noise varies with the squeezing parameter at the opposite of the photon noise, namely, if one decreases, the other increases and vice versa; thus, an optimum regime must be found. In the context of our proposal the behavior is similar, but for reasonable values of the involved parameters RP noise is completely negligible (justifying our perturbative approach). Figure 3 shows how RP noise starts to affect the uncertainty for an average coherent field intensity $\mu \gtrsim 10^{23}$ for $\tau = 10^{-3}$ s (the photons introduced by the quantum modes are negligible), which is a power larger than $\hbar\omega\mu/\tau = 3.3 \times 10^7$ W. Since the HN must be sought in the region of the MHz, i.e., for a short measurement time ($\tau \approx 10^{-6}$ s), the RP contribution would be significant for power values larger than 10^{13} W, a value well far away from the current and future interferometry technology. One can be surprised that in the present scheme the radiation pressure is negligible, while it is not always the case for the standard phase measurement involving a single interferometer. However, we stress that here we are measuring a phase covariance between two interferometers, instead of the phase values in single ones.

In conclusion, in addition to our analysis concerning the use of two independent squeezed states, which substantially confirms the advantages already demonstrated for gravity wave detection, the investigation carried out exploiting entanglement leads to the unprecedented result that, in an ideal situation, the background noise can be completely washed out. This achievement not only paves the way for reaching much higher sensibility in the holometer under construction at Fermilab or for the realization of a tabletop experiment to test quantum gravity, but also sheds some first light on new unexpected opportunities offered by the use of quantum states of light for a fundamental reduction of noise in interferometric schemes.

The research leading to these results has received funding from the EU FP7 under Grant Agreement No. 308803

(BRISQ), Fondazione San Paolo, and MIUR (FIRB "LiCHIS" – RBFR10YQ3H and Progetto Premiale "Oltre i limiti classici di misura"), NATO Grant No. EAP-SFPP98439.

[1] G. A. Camelia, J. Ellis, N. E. Mavromatos, D. V. Nanopoulos, and S. Sarkar, Nature (London) **393**, 763 (1998).

[2] G. A. Camelia, Nature (London) **398**, 216 (1999).

[3] G. A. Camelia, Nature (London) **478**, 466 (2011).

[4] I. Pikovski, M. R. Vanner, M. Aspelmeyer, M. S. Kim, and Č. Brukner, Nat. Phys. **8**, 393 (2012).

[5] G. Hogan, Phys. Rev. D **85**, 064007 (2012).

[6] J. D. Bekenstein, Phys. Rev. D **86**, 124040 (2012).

[7] P. Aschieri and L. Castellani, J. Geom. Phys. **60**, 375 (2010).

[8] P. Aschieri and L. Castellani, J. High Energy Phys. 06 (2009) 086.

[9] www.holometer.fnal.gov, accessed 03/23/2012.

[10] K. Banaszek, R. Demkowicz-Dobrzański, and I. A. Walmsley, Nat. Photonics **3**, 673 (2009).

[11] V. Giovannetti, S. Lloyd, and L. Maccone, Nat. Photonics **5**, 222 (2011).

[12] S. F. Huelga, C. Macchiavello, T. Pellizzari, A. Ekert, M. Plenio, and J. Cirac, Phys. Rev. Lett. **79**, 3865 (1997).

[13] H. Lee, P. Kook, and J. Dowling, J. Mod. Opt. **49**, 2325 (2002).

[14] G. Brida, M. Genovese, and I. Ruo Berchera, Nat. Photonics **4**, 227 (2010).

[15] E. D. Lopaeva, I. Ruo Berchera, I. P. Degiovanni, S. Olivares, G. Brida, and M. Genovese, Phys. Rev. Lett. **110**, 153603 (2013).

[16] R. Schnabel, N. Mavalvala, D. E. McClelland, and P. K. Lam, Nat. Commun. **1**, 121 (2010).

[17] C. M. Caves, Phys. Rev. D **23**, 1693 (1981).

[18] K. McKenzie, D. Shaddock, D. McClelland, B. Buchler, and P. Lam, Phys. Rev. Lett. **88**, 231102 (2002).

[19] Abadie *et al.*, Nat. Phys. **7**, 962 (2011).

[20] The $\|$ configuration is realized by placing side by side the arms of the two interferometers, while the $\perp$ configuration is implemented in the Fermilab holometer by rotating one of the interferometers by 90° [9], as sketched in Fig. 1(b).

[21] See Supplemental Material at http://link.aps.org/supplemental/10.1103/PhysRevLett.110.213601 for further details and demonstrations.

[22] Another useful interpretation of this quantity is related to the SNR of the measurement. In general, $\mathrm{SNR} \equiv S/\sqrt{\mathrm{Var}(S)} = (KE)/\sqrt{\mathrm{Var}(S)}$, where S is the signal ($S = \mathcal{E}_{\|}[\hat{C}] - \mathcal{E}_{\perp}[\hat{C}]$ for us) that in a linear approximation is related by a certain constant K [K is the denominator of Eq. (2)] to the quantity under estimation E, in our case the phase covariance $E = \mathcal{E}_{\|}[\delta\phi_1\delta\phi_2]$. The minimum resolvable value of E, i.e., the one that allows one to reach a SNR larger than 1, is $E_{\mathrm{min}} = \sqrt{\mathrm{Var}(S)}/K$, i.e., exactly $\mathcal{U}$.

[23] L. Mandel and E. Wolf, *Optical Coherence and Quantum Optics* (Cambridge University Press, Cambridge, England, 1995).

[24] S. Olivares, Eur. Phys. J. Special Topics **203**, 3 (2012).

[25] G. Brida, M. Genovese, A. Meda, and I. Ruo Berchera, Phys. Rev. A **83**, 033811 (2011).

[26] M. Bondani, A. Allevi, G. Zambra, M. G. A. Paris, and A. Andreoni, Phys. Rev. A **76**, 013833 (2007).

[27] T. Iskhakov, M. V. Chekhova, and G. Leuchs, Phys. Rev. Lett. **102**, 183602 (2009).

[28] V. B. Braginsky and F. Y. Khalili, Rev. Mod. Phys. **68**, 1 (1996).

[29] H. J. Kimble, Y. Levin, A. B. Matsko, K. S. Thorne, and S. P. Vyatchanin, Phys. Rev. D **65**, 022002 (2001).

[30] According to Ref. [22], we have $\mathrm{SNR}_{\mathrm{TWB/SQ}}/\mathrm{SNR}_{\mathrm{CL}} = K_{\mathrm{TWB/SQ}}/K_{\mathrm{CL}}(\mathrm{Var}(S_{\mathrm{CL}})/\mathrm{Var}(S_{\mathrm{TWB/SQ}}))^{1/2} = \mathcal{U}_{\mathrm{CL}}/\mathcal{U}_{\mathrm{TWB/SQ}}$; thus, Fig. 3 represents also the inverse of the SNR normalized to the classical benchmark.